Vegetation Dynamics Enhancing Long-Term Climate Variability Confirmed by Two Models

CHRISTINE DELIRE

Groupe d'Etude de l'Atmosphère Météorologique, URA 1357 GAME/CNRM, CNRS/Météo-France, Toulouse, France

NATHALIE DE NOBLET-DUCOUDRÉ

Laboratoire des Sciences du Climat et de l'Environnement, Unité Mixte CEA-CNRS-UVSQ, Gif-sur-Yvette, France

ADRIANA SIMA* AND ISABELLE GOUIRAND+

Institut des Sciences de l'Evolution-Montpellier, Unité Mixte UMII/CNRS, Université Montpellier II, Montpellier, France

(Manuscript received 8 February 2010, in final form 14 December 2010)

ABSTRACT

Two different coupled climate–vegetation models, the Community Climate Model version 3 coupled to the Integrated Biosphere Simulator (CCM3–IBIS) and the Laboratoire de Météorologie Dynamique's climate model coupled to the Organizing Carbon and Hydrology in Dynamic Ecosystems model (LMDz–ORCHIDEE), are used to study the effects of vegetation dynamics on climate variability. Two sets of simulations of the preindustrial climate are performed using fixed climatological sea surface temperatures: one set taking into account vegetation cover dynamics and the other keeping the vegetation cover fixed. Spectral analysis of the simulated precipitation and temperature over land shows that for both models the interactions between vegetation dynamics and the atmosphere enhance the low-frequency variability of the biosphere–atmosphere system at time scales ranging from a few years to a century. Despite differences in the magnitude of the signal between the two models, this confirms that vegetation dynamics introduces a long-term memory into the climate system by slowly modifying the physical characteristics of the land surface (albedo, roughness evapotranspiration).

Unrealistic modeled feedbacks between the vegetation and the atmosphere would cast doubts on this result. The simulated feedback processes in the models used in this work are compared to the observed using a recently developed statistical approach. The models simulate feedbacks of the right sign and order of magnitude over large regions of the globe: positive temperature feedback in the mid- to high latitudes, negative feedback in semiarid regions, and positive precipitation feedback in semiarid regions. The models disagree in the tropics, where there is no statistical significance in the observations. The realistic modeled vegetation–atmosphere feedback gives us confidence that the vegetation dynamics enhancement of the long-term climate variability is not a model artifact.

1. Introduction

At regional to global scales the distribution of terrestrial ecosystems, as well as their structure and function, strongly depend on climate (Prentice et al. 1992). The link between climate and vegetation was already known in ancient Greece (Woodward 1987) and further studied in the nineteenth and twentieth centuries. More recently, it has been shown mainly through modeling work that vegetation itself could affect the atmospheric circulation through biophysical processes. Vegetation affects the land surface albedo and thereby determines the amount of net radiation available for heating the ground and the lower atmosphere, as well as for evaporating water. Through their rooting system and their stomatal control on transpiration, plants also strongly affect evapotranspiration and the partitioning between latent and sensible heat fluxes. Finally, the height and density of the vegetation affect the roughness of the land

* Current affiliation: Ecole Normale Supérieure, Laboratoire de Météorologie Dynamique and CERES-ERTI, Paris, France.

+ Current affiliation: Department of Biological and Chemical Sciences, University of the West Indies, Bridgetown, Barbados.

Corresponding author address: Christine Delire, GMGEC, Météo-France, 42 av. G. Coriolis, 31057 Toulouse CEDEX, France.
E-mail: christine.delire@meteo.fr

DOI: 10.1175/2010JCLI3664.1

surface, which influences the mixing of air close to the surface thereby influencing sensible and latent cooling processes.

Most of the early modeling work on the biophysical influence of vegetation on climate focused on tropical regions, studying either desertification [starting with Charney et al. (1975, 1977)], deforestation (e.g., Dickinson and Henderson-Sellers 1988; Dorman and Sellers 1989; Lean and Warrilow 1989; Nobre et al. 1991; Hahmann and Dickinson 1997; Snyder et al. 2004 a,b), or the greening of desert landscapes during the Holocene (Kutzbach et al. 1996; Texier et al. 1997; Brovkin et al. 1998; de Noblet-Ducoudré et al. 2000). Other studies also looked at the effects of changing vegetation cover in the mid- to high latitudes (e.g., Bonan et al. 1992, 1995; Bonan 1997, 1999; Douville and Royer 1997; Levis et al. 1999) or at the effects of realistic land-use changes on the climate (Chase et al. 2000; Bounoua et al. 2002; Pielke et al. 2002; Ramankutty et al. 2006; Voldoire et al. 2007; Pitman et al. 2009).

All these studies addressed the effects of a fixed imposed change in vegetation cover on the mean climate. But vegetation cover changes continually over time in response to climate variability. Changes happen at time scales ranging from seasons (for leaf area) to years and even decades (for vegetation structure and community composition). Because vegetation affects the water, energy, and momentum balance at the land surface, vegetation dynamics may be capable of producing long-term variability in the climate system. This hypothesis was first studied in semiarid areas where vegetation is water limited, like the Sahel. Over the past few centuries, the climate of the Sahel has been characterized by a succession of multidecadal dry and wet periods. In the rest of the world, however, wet and dry spells do not usually exceed 2–5 yr (Nicholson 2000). In a review of observational and modeling work, Nicholson (2000) showed how vegetation modulates land–atmosphere interactions by accelerating or delaying moisture transfer to the atmosphere. With models of intermediate complexity, Zeng et al. (1999) and Wang and Eltahir (2000a; 2000b) showed that a change in the Atlantic sea surface temperatures (SSTs) off the coast of West Africa or an increase in land degradation in the Sahel (Wang and Eltahir 2000b,c) alone are not sufficient to cause the persistent drought observed in the region from the 1970s until recently, unless local feedbacks from slow changes in the vegetation cover are included.

With a general circulation model (GCM) coupled to a dynamic vegetation model [i.e., the CCM3–IBIS; Delire et al. (2002)], and forced by climatological sea surface temperatures, Delire et al. (2004) found that dynamic interactions between the atmosphere and vegetation enhance precipitation variability on land at time scales from a decade to a century. These interactions introduce persistent precipitation anomalies in several ecological transition zones: between forest and grasslands in the North American Midwest, in South Africa, at the southern limit of the tropical forest in the Amazon Basin, and between the savanna and desert in the Sahel, Australia, and in portions of the Arabian Peninsula. In a similar study centered on the Sahel region, Wang et al. (2004), using the same vegetation model coupled to the Global Environmental and Ecological Simulation of Interactive Systems (GENESIS) climate model, showed that vegetation dynamics act as a mechanism of persistence for regional climates. On the other hand, Crucifix et al. (2005), using version 3 of the Hadley Centre's Slab Model (HadSM3) coupled to a slab-ocean model, found weak impacts of vegetation dynamics on precipitation variability despite the strong influence of vegetation dynamics on the surface latent and sensible heat flux interannual variabilities.

Observations of vegetation feedbacks on the atmosphere at large scales are mostly based on the cross analysis (with lags) of the climate record and the satellite-derived normalized difference vegetation index (NDVI) record, giving the evolution over time of vegetation greenness. Lotsch et al. (2003) showed extensive patterns of joint NDVI–precipitation variability at seasonal scales, suggesting strong climate–biosphere coupling. Liu et al. (2006) proposed a method of estimating the strength of the vegetation–atmosphere feedback using an approach designed at first to assess ocean–atmosphere feedbacks (Frankignoul et al. 1998). Using monthly averaged data, they found that the feedback of vegetation on temperature is important in the mid- and high latitudes. It is mostly positive and can explain 10%–25% of the temperature variability in some regions. The feedback of vegetation on precipitation happens mostly in the tropics and subtropics, is much smaller, and explains only 5% of the observed precipitation variance. Using a different statistical technique and seasonally binned NDVI data available for circa 20 yr, Alessandri and Navarra (2008) showed that 19% of the vegetation variance is forced by precipitation while 12% of the precipitation variance is forced by vegetation. They also found that the component of rainfall variability forced by the vegetation is linked to El Niño–Southern Oscillation cycles, with the vegetation acting as a biophysical memory of ENSO.

Here, we compare the effects of vegetation dynamics of two completely different coupled atmospheric–vegetation models, as mentioned above: CCM3–IBIS and LMDz–ORCHIDEE. We are motivated by the contradiction between Crucifix et al. (2005), who did not find any significant effects of vegetation dynamics on climate variability with HadSM3 coupled to Top-down Representation of Interactive Foliage and Flora Including Dynamics (TRIFFID) vegetation model, and Delire et al. (2004)

and Wang et al. (2004), who did find a significant effect but were using the same vegetation model, IBIS. Using identical settings, we analyze the two model results and try to identify similar patterns of behavior and discrepancies in the simulations of vegetation atmosphere feedback processes and the effects of vegetation dynamics on climate variability. We focus our study on the biophysical feedbacks, neglecting the biogeochemical feedbacks of the terrestrial ecosystems on the atmosphere (see Foley et al. 2003 for a review). Our conclusions regarding the effects of vegetation dynamics on climate variability could be questioned if the simulated vegetation–atmosphere feedbacks were unreasonable. Therefore, we check for the realism of these feedbacks by comparing the vegetation–atmosphere feedback efficiency simulated by the two models to the feedback efficiency derived from data using the approach of Liu et al. (2006).

Our experimental protocol and chosen diagnostics are designed to address the following questions:

- Do vegetation dynamics enhance long-term climate variability in these models?
- Are the simulated vegetation feedbacks reasonable in comparison to the observations? What fraction of the precipitation and temperature variance is explained by vegetation feedbacks? How does this compare to recent conclusions derived from observations?

2. The two coupled atmosphere–vegetation models

a. CCM3–IBIS

CCM3–IBIS is the National Center for Atmospheric Research's Community Climate Model, version 3 (CCM3; Kiehl et al. 1998), coupled with the updated Integrated Biosphere Simulator (IBIS) land surface model (Foley et al. 1996; Kucharik et al. 2000).

CCM3 simulates the large-scale physics (radiative transfer, hydrologic cycle, cloud development, thermodynamics) and dynamics of the atmosphere. In this study we operate the model at a spectral resolution of T42 (~2.8° × 2.8° grid), with 18 levels in the vertical and a 20-min time step.

The global terrestrial biosphere model IBIS (version 2) simulates land surface physics, canopy physiology, plant phenology (budburst and senescence), vegetation dynamics (accumulation and turnover of carbon, and simple competition between plant functional types), and carbon cycling. Land surface physics and canopy physiology are calculated with the atmospheric model time step (20 min). The plant phenology algorithm has a daily time step and the vegetation dynamics are solved with an annual time step. In these simulations, IBIS operates on the same T42 spatial grid as the CCM3 atmospheric model.

The land surface module in IBIS describes two vegetation layers (i.e., "trees" and "grasses and shrubs") and six soil layers, to simulate soil temperature, soil water, and soil ice content over a total depth of 4 m. Physiologically based formulations of C3 and C4 photosynthesis (Farquhar et al. 1980; Collatz et al. 1992), stomatal conductance (Collatz et al. 1991), and respiration (Amthor 1984) are used to simulate canopy gas exchange processes. Budburst and senescence depend on climatic factors adapted from the empirical algorithm presented by Botta et al. (2000). The vegetation dynamics module calculates the evolution of 12 plant functional types (PFTs) that differ in their form (trees, shrubs, grasses), leaf type (broadleaf or needleleaf), patterns of leaf display (evergreen or deciduous), photosynthetic pathway (C3 or C4), and climate zone (tropical, temperate, boreal). A simple set of climatic limits (growing degree-day requirements, cold tolerance limits, and minimum chilling requirements) determines where each PFT is allowed to grow. The climatically viable PFTs compete for light and water and their relative abundance in each grid cell is based on the annual carbon balance. Competition between grass types or between tree types results from differences in carbon allocation, phenology, leaf type, or photosynthetic pathway. The version of IBIS used here does not include nitrogen limitations.

IBIS has been tested against site-specific biophysical measurements from flux towers (Delire and Foley 1999) and field-level ecological studies (Kucharik et al. 2001; Senna et al. 2005; Kucharik et al. 2006), as well as spatially extensive ecological (Kucharik et al. 2000) and hydrological data (Costa and Foley 1997; Lenters et al. 2000). It is used to study the climate, hydrology, and vegetation of tropical South America (Coe et al. 2002; Costa et al. 2007; Senna et al. 2009; Coe et al. 2009).

IBIS was coupled to a variety of climate models: the GENESIS GCM (Levis et al. 1999; 2000), an intermediate complexity model (Wang and Eltahir 2000a), and version 3 of the Regional Climate Model (RegCM3; Winter et al. 2009). The CCM3–IBIS simulated climate and terrestrial carbon cycles were analyzed in Delire et al. (2002, 2003).

b. LMDz–ORCHIDEE

LMDz (Hourdin et al. 2006) is the atmospheric component of the Institut Pierre Simon Laplace's (IPSL) climate model (Marti et al. 2010). It is run at a resolution of 3.75° × 2.5°, with 19 levels in the vertical.

The dynamic global vegetation model ORCHIDEE (Krinner et al. 2005) consists of the Schématisation des Échanges Hydriques à l'Interface Biosphere–Atmosphère surface–vegetation–atmosphere transfer scheme (SECHIBA; Ducoudré et al. 1993; De Rosnay and Polcher 1998) and of the Saclay–Toulouse–Orsay Model

for the Analysis of Terrestrial Ecosystems carbon module (STOMATE), which includes the dynamic vegetation component of the Lund–Potsdam–Jena (LPJ) dynamic model (Sitch et al. 2003). SECHIBA calculates processes characterized by short time scales, ranging from a few minutes to hours, such as energy and water exchanges between the atmosphere and the terrestrial biosphere, photosynthesis, as well as the soil water budget. SECHIBA has a time step similar to that of the atmosphere's physics (30 min) in order to simulate the diurnal cycle of the terrestrial biosphere. STOMATE treats daily processes such as carbon allocation, litter decomposition, soil carbon dynamics, phenology, maintenance, and growth respiration. Important parameterizations, allowing the dynamic simulation of vegetation distribution, have been taken from the LPJ global model: processes such as fire, sapling establishment, light competition, tree mortality, and climatic criteria for the introduction and elimination of plant functional types are integrated into ORCHIDEE, with a time step of 1 yr. To avoid jumps on 1 January, the distribution of vegetation is updated every day, using climatological and productivity variables smoothed over the preceding year. ORCHIDEE describes the land surface as a mosaic of 12 PFTs, as well as bare soil. The definition of a PFT is based on ecological parameters such as plant physiognomy (tree or grass), leaves (needleleaf or broadleaf), phenology (evergreen, summergreen, or raingreen) and photosynthesis type for crops and grasses (C3 or C4). Relevant biogeochemical parameters are prescribed for each PFT (Krinner et al. 2005). In the current version of ORCHIDEE there is no explicit terrestrial nitrogen cycle. However, nitrogen is implicitly taken into account in the photosynthesis and carbon allocation calculations. For the carbon allocation, a nitrogen limitation is parameterized as a function of monthly soil moisture and temperature, implicitly representing the dependence of nitrogen availability on the microbial activity in soil. Photosynthesis is parameterized as an exponentially decreasing function of canopy depth with an asymptotic minimum limit of 30% of the maximum efficiency, to take into account the vertical variation of the photosynthetic capacity based on the leaf nitrogen content. Leaf onset and senescence are calculated, depending on the PFT, by applying warmth and/or moisture stress criteria to the meteorological conditions. Carbon allocation to leaves, and to other compartments such as roots and sapwood, depends on external constraints such as temperature, moisture, or light.

The ORCHIDEE model has been widely used to assess the transient impacts of climate change on the global or regional water and carbon cycles (Vérant et al. 2004; Ngo-Duc et al. 2005a,b; Ciais et al. 2005; Piao et al. 2007). The seasonal cycles of energy and water exchanges and carbon fluxes from the ORCHIDEE model have been extensively calibrated and validated against eddy covariance data from a number of field sites (Krinner et al. 2005; Morales et al. 2005). The interannual variability in LAI over the recent period is also realistically represented when compared to satellite-derived data (Piao et al. 2006).

A summary of the similarities and dissimilarities of the IBIS and ORCHIDEE vegetation models is presented in Table 1.

3. Design of numerical experiments

We chose to test the effects of vegetation dynamics on long-term climate variability for preindustrial conditions. We performed two simulations of the global climate with each model: one in which vegetation cover is predicted and interacts with climate, and the other with the vegetation cover fixed. We will refer to the first simulations as the dynamic vegetation simulations (DYN) and the second simulations as the fixed vegetation simulations (FIX).

We chose to impose fixed climatological sea surface temperatures (SSTs) to isolate the effects of vegetation dynamics on the atmosphere. We used the average seasonal cycle of the period 1870–99 from the Hadley Centre Global Sea Ice and Sea Surface Temperature (HadISST) dataset (Rayner et al. 2003). Using fixed SSTs allows us to remove the interannual variability associated with the ocean and to guarantee that the differences in climate variability between dynamic and fixed vegetation simulations are due only to the interaction between the dynamic vegetation cover and the atmosphere. We are aware that by prescribing SSTs we miss the coupled land–ocean–atmosphere interactions that play a role in climate variability (see, e.g., Alessandri and Navarra 2008). However, we are confident that by isolating the sole effect of vegetation dynamics on atmospheric variability we can capture some major mechanisms by which vegetation dynamics affect long- (short-) term variability, even though the magnitude of the simulated influence may be under- (over-) estimated compared to the coupled atmosphere–ocean–vegetation system.

Both models were first run to equilibrium for preindustrial conditions [modern orbital conditions, 1365 W m^{-2} solar constant, 280 ppmv of CO_2, 760 ppb of CH_4, 270 ppb of N_2O, and no CFCs; see for instance Solomon et al. (2007, chapter 2)] in dynamic vegetation mode. We ran CCM3–IBIS for 400 yr using as initial conditions the vegetation distribution simulated by an unpublished 200-yr preindustrial run. The LMDz–ORCHIDEE model was run for 980 yr starting from bare ground. We used the last 300 yr of each run for our analyses. The LMDz–ORCHIDEE model had to be run longer than CCM3–IBIS to reach equilibrium partly because ORCHIDEE started from bare earth (while IBIS started

TABLE 1. Main processes accounted for in both DGVMs. The major differences identified are highlighted in boldface.

Characteristics	DGVM	IBIS	ORCHIDEE
Biogeography	No. of natural PFTs	12	10 (excluding bare ground)
	No. of vegetation layers	Two: high and low	One (herbaceous type cannot be shaded by trees)
	Subgrid-scale heterogeneity	Two homogeneous canopies with a mix of up to eight (four) PFTs for the upper (lower) canopies	Separate tile for each PFT (all PFTs can coexist within the same grid cell)
Soil physics		Darcy's law and heat equation solved in six layers	Two layers (Ducoudré et al. 1993; de Rosnay and Polcher 1998)
Canopy physics	Radiation	Two-stream approximation for two canopies	Two-stream approximation per PFT to compute surface albedo
	Energy balance	Separate energy balance for two canopies and soil	Only one energy budget per grid cell based on the averaged surface albedo
Canopy physiology	Photosynthesis	Farquhar et al. (1980); Collatz et al. (1992); Collatz et al. (1991) for stomatal conductance	Farquhar et al. (1980); Collatz et al. (1992); Ball et al. (1987) for stomatal conductance
Time step for all above		20 min	30 min
Phenology		Shape of seasonal cycle based on climate (Botta et al. 2000); peak LAI per PFT results from previous year's carbon balance in DYN mode	Leaf onset and senescence climatically based following Botta et al. (2000); foliar growth results from carbon balance and allocation
Time step		Daily	Daily
Vegetation dynamics	**Establishment**	Not represented; all PFTs can grow anywhere if within bioclimatic limits	As in LPJ (Sitch et al. 2003)
	Growth	Solely based on PFT carbon balance	LPJ (based on allometric relations)
	Mortality	Constant fraction of living biomass	Constant fraction of living biomass
Time step		Yearly	Updated daily but smoothed by preceding year's values
Perturbations	**Fire**	None	Based on Thonicke et al. (2001)
Other model characteristics	Main surface variables (derived from prognostically computed biomass pools)	LAI for each PFT; upper and lower canopy coverage; upper and lower canopy height; derived parameters (albedo, roughness length etc.)	LAI; roughness length; surface albedo; maximum vegetation coverage
	Fixed vegetation mode	Fixed vegetation coverage Fixed mix of PFT; fixed peak LAI per PFT Fixed carbon pools	Fixed vegetation coverage; variable peak LAI per PFT based on the carbon cycle; computation of all carbon pools

with a reasonable vegetation map), and calculated annual fires (section 2) that impacted the fraction of PFTs and slowed down the establishment of equilibrium vegetation.

In the fixed-vegetation simulations, we imposed on the coupled atmosphere–vegetation models a constant vegetation cover obtained by averaging the vegetation characteristics of the last 50 yr of the corresponding dynamic vegetation run. Both models were run for 200 yr in FIX mode and the last 150 yr were analyzed.

Fixed vegetation has a somewhat different meaning in the two coupled AGCM–vegetation models. In the case of CCM3–IBIS, prescribing the vegetation means that the relative abundance of the 12 plant functional types is fixed in each grid cell. All the carbon pools are identical from one year to the next, and the annual mean vegetation cover and the peak LAI reached during the year are constant. Budburst, leaf growth, and senescence, however, still depend on the climate during the course of the

year. The amplitude of the seasonal cycle of LAI is thus identical each year, but its shape varies from year to year according to the climate. This variability in the seasonal cycle of leaf display affects the atmosphere. At shorter time scales (hourly, daily), vegetation also reacts directly to changes in the atmosphere. For example, transpiration is reduced in periods of drought. Feedbacks between the vegetation and the atmosphere are thus not completely neglected: they are taken into account at short time scales (hourly daily) and during the seasonal cycle of leaf phenology, but not for year-to-year variations in canopy cover and vegetation structure. In the case of LMDz–ORCHIDEE, short time scales are also taken into account but, contrary to CCM3–IBIS, carbon pools are updated each day even when the vegetation cover is prescribed (Krinner et al. 2005). The fractional cover and the maximum LAI of a PFT do not change from year to year, but depending on the carbon cycle, the maximum LAI might not necessarily be reached. Therefore, in contrast to CCM3–IBIS, the amplitude of the seasonal cycle of LAI may vary from year to year.

4. Mean state and variability of climate and vegetation

a. Climate

The mean climate simulated by CCM3–IBIS in this study is very similar to the one described in Delire et al. (2003, Fig. 2), despite the higher resolution (T42 instead of T31) and differing conditions (preindustrial versus present day). Therefore, we only briefly present it here; maps and details can be found in Delire et al. (2003). Compared to the present-day climatology from New et al. (2002), the model tends to underestimate the boreal summer 2-m temperature in Alaska and Siberia, while overestimating it in Greenland, the United States, eastern Canada, the Mediterranean region, and the Amazon. Boreal winter is characterized by an overall warm bias over the mid- to high northern latitudes and a cold bias around the North Atlantic. Precipitation amounts are overestimated in Africa, the Arabian Peninsula, and central China, and underestimated in the southern United States, northern South America, around the Gulf of Guinea, and Indonesia.

The mean climate simulated in this study by LMDz–ORCHIDEE is similar to the preindustrial climate simulation for the Intergovernmental Panel on Climate Change's (IPCC) Fourth Assessment Report (AR4) without dynamic vegetation (information online at http://dods.ipsl.jussieu.fr/omamce/IPSLCM4/DocIPSLCM4/FILES/DocIPSLCM4_color.pdf). Precipitation is too low over northern India, northern Australia, and most of South America, while it is too great in central Africa, the Indonesian Archipelago, central China, Alaska, and the Andes. Temperatures in boreal winter are too cold over most land areas with the exception of Alaska, northeast Siberia, the Andes, and a band stretching from the Mediterranean Sea to Lake Baikal. In boreal summer, the model tends to simulate an overall warm bias over North America and Eurasia, and over the Amazon Basin. Southeastern South America, most of Africa, China, and Australia are too cold. Maps and details can be found on the Web site cited above.

b. Mean vegetation distribution

The vegetation in equilibrium with these two simulated climates is presented in Fig. 1 together with the observations derived from the 1982–94 Advanced Very High Resolution Radiometer (AVHRR) dataset and analyzed by DeFries et al. (2000). We show the mean foliage projected cover (FPC) for the last 50 yr of each DYN run. The FPC is defined as the fraction f occupied by the PFT in the grid cell multiplied by a function of its LAI: $f[1-\exp(-k \times \mathrm{LAI})]$. The function represents the fraction of radiation transmitted by the canopy according to Beer's law with an extinction coefficient k. The ability of the offline versions of the vegetation models to represent the geographic patterns of vegetation has been discussed earlier [Kucharik et al. (2000) for IBIS and Krinner et al. (2005) for ORCHIDEE]. Delire et al. (2003) also compared the impacts of coupling land and atmosphere on the simulated vegetation for present-day climate conditions and highlighted the areas where discrepancies in the simulated atmospheric variables are amplified by dynamic vegetation.

The two models simulate the gross features of the distribution of vegetation types on the surface of the earth: evergreen and deciduous forests in the northern mid- to high latitudes, and evergreen forests around the equator with deciduous forests surrounding them in the case of CCM3–IBIS. In LMDz–ORCHIDEE there are very few deciduous trees in the tropics, and they are collocated with evergreen forests. Grasses (together with shrubs in the case of CCM3–IBIS) are found in the Arctic, the western United States, the Mediterranean, and the Middle East; as well as in the Sahel; and in Australia. The sum of tree, grass, and shrub FPCs never exceeds one in LMDz–ORCHIDEE while it can exceed this value in the case of CCM3–IBIS, which allows two canopy layers to coexist (grasses and shrubs in the lower canopy and trees in the upper canopy).

Both models tend to underestimate low vegetation cover compared to DeFries et al. (2000). One obvious reason is that human activity was not taken into account in these model simulations while the DeFries et al. dataset reflects the state of the vegetation between 1983 and 1994 and includes croplands and pastures in the low vegetation

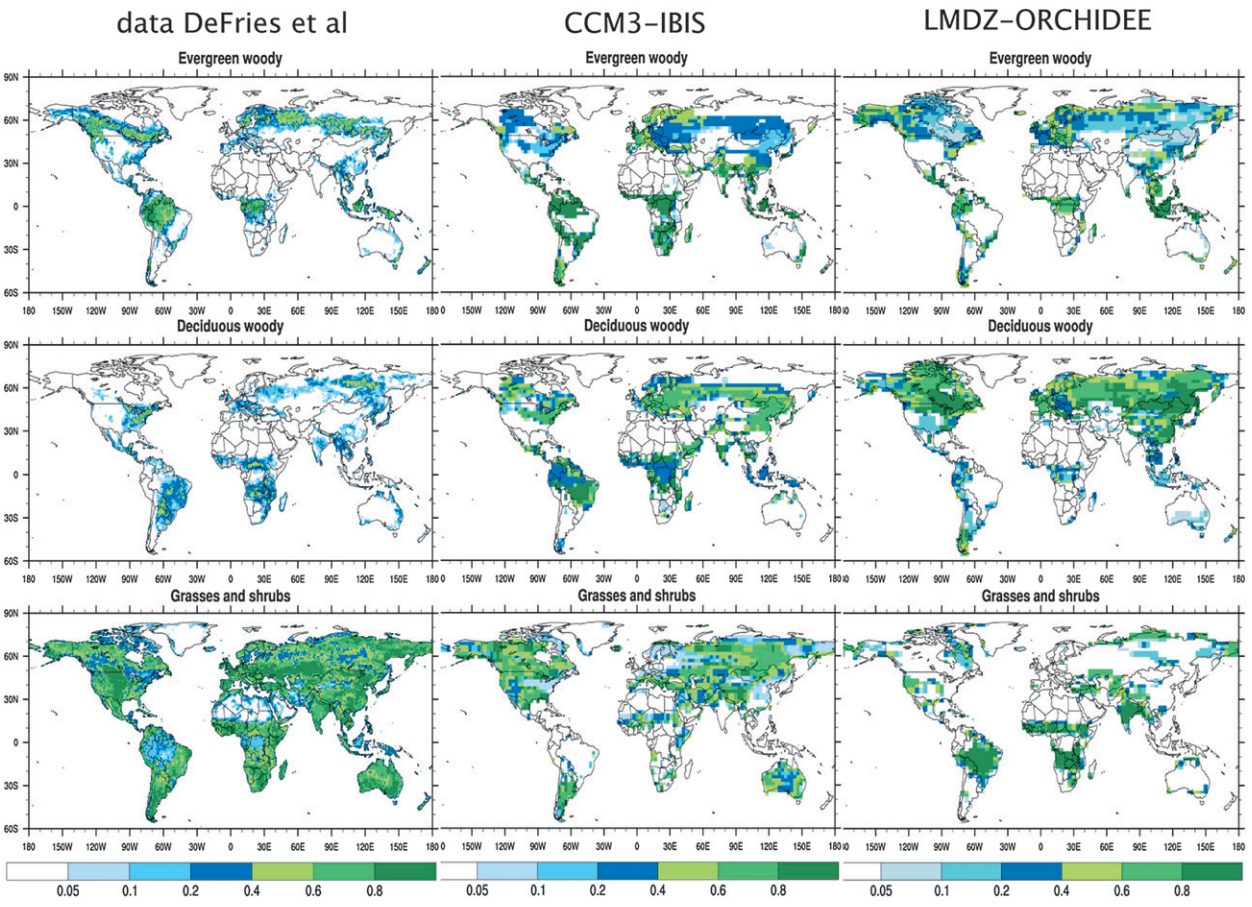

FIG. 1. (left) Fraction of vegetation cover deduced from AVHRR satellite data shown at 1° × 1° resolution (DeFries et al. 2000), and mean radiative foliage projected cover simulated by (middle) CCM3–IBIS and (right) LMDz–ORCHIDEE, for (top) evergreen trees, (middle) deciduous trees, and (bottom) grasses plus shrubs.

category. Additionally, vegetation cover may be overestimated in arid regions by the DeFries et al. product (Tian et al. 2004; Zeng et al. 2000).

The models present biases in the simulated vegetation. Some biases are due to the vegetation model itself while others result from the atmospheric model and can be enhanced by feedbacks between vegetation and the atmosphere (Delire et al. 2003). CCM3–IBIS underestimates forest cover in Alaska and northeast Siberia and favors deciduous trees at the expense of evergreen trees in most of the temperate and boreal forests of Eurasia and North America. The lack of forest cover in northern Siberia and Alaska is linked to a cold bias simulated by the atmospheric model in the summer over these regions (Delire et al. 2002, 2003). On the other hand, the dominance of deciduous trees at the expense of evergreens in temperate and boreal forests is due to the vegetation model IBIS. We obtain the same bias when IBIS is forced by observed climate data (see Delire et al. 2003, Fig. 3) and is partly due to an imperfect representation of deciduous leaf phenology (Givnish 2002).

The LMDz–ORCHIDEE model tends to overestimate forest cover at high latitudes in the Northern Hemisphere. The model simulates deciduous forest in the Arctic northwest of Hudson Bay and in northeast Siberia because a small warm bias in the summer months in the atmospheric model allows the tree line to move north. The higher tree cover feeds back to the climate and enhances the original bias. Like CCM3–IBIS, LMDz–ORCHIDEE simulates more deciduous than evergreen trees in the temperate and boreal forests of Eurasia and North America. But here the bias cannot be traced to the vegetation model (as with CCM3–IBIS). Indeed, when forced with the observed climatology, ORCHIDEE tends to overestimate the area covered with evergreen trees and underestimate the deciduous forest in the mid- to high northern latitudes (cf. Krinner et al. 2005).

In the tropics, CCM3–IBIS overestimates forest cover in Africa and the Arabian Peninsula. The simulated lush vegetation in the Arabian Peninsula with CCM3–IBIS is a result of a positive precipitation bias in the atmospheric model that is enhanced by vegetation feedbacks

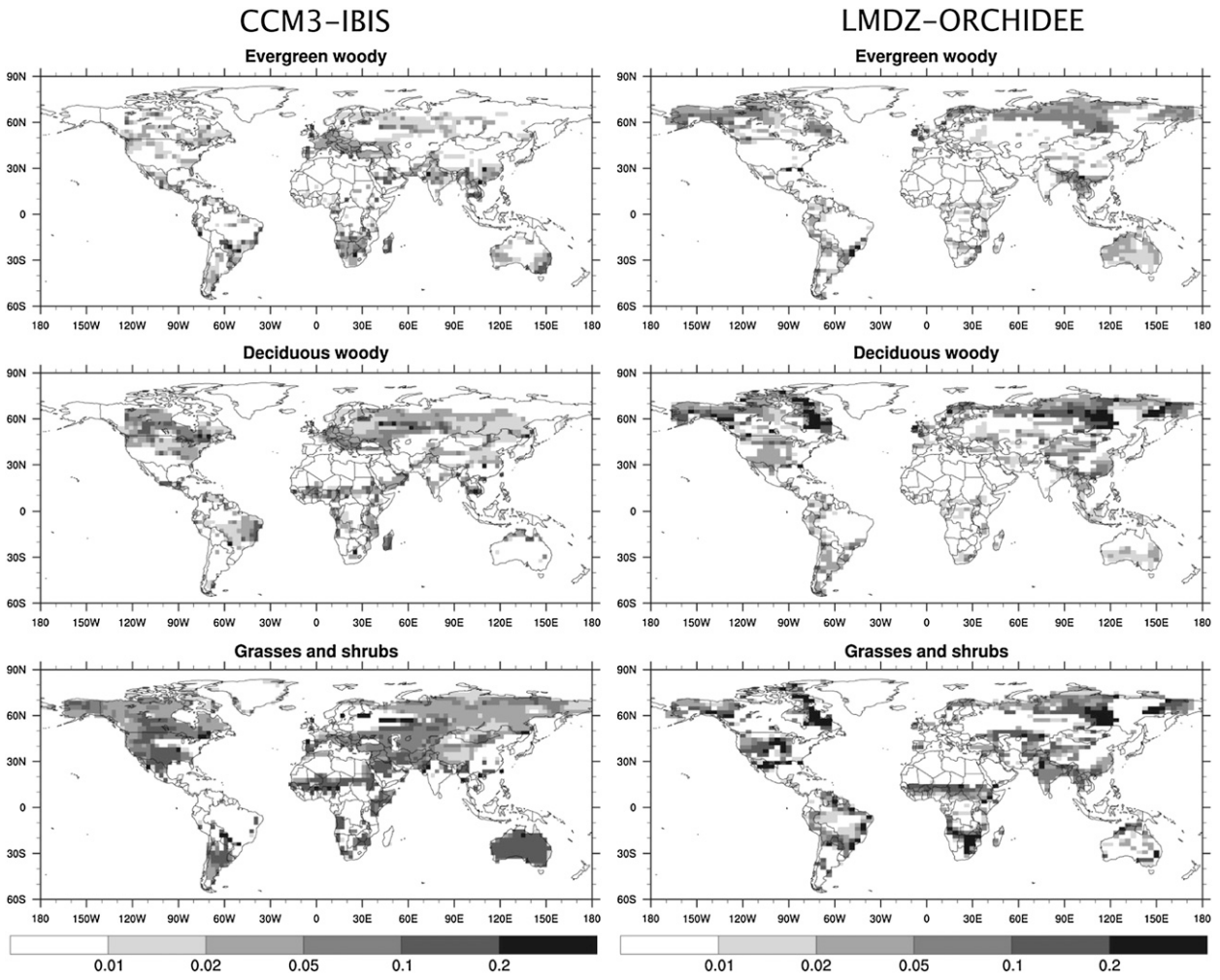

FIG. 2. Standard deviation of the mean foliage projected cover simulated by (left) CCM3–IBIS and (right) LMDz–ORCHIDEE, for (top) evergreen trees, (middle) deciduous trees, and (bottom) grasses plus shrubs.

(Delire et al. 2003). The LMDz–ORCHIDEE model underestimates convective activity over South America (Hourdin et al. 2006). The simulated precipitation is too weak year round over the Amazon Basin to sustain a tropical rain forest. As a result, a mix of C3 and C4 grasses covers the basin, which further enhances the original negative precipitation bias.

The lack of an Amazon rain forest is a fairly common problem in coupled atmosphere–ocean–vegetation models. Thompson et al. (2004) using CCM3–IBIS coupled to a dynamic ocean model had to incorporate a precipitation correction method to sustain the Amazonian forest under present-day climate conditions. Similarly, Cox et al. (2000) simulated a complete loss of the Amazonian forest by 2050 using a coupled atmosphere–ocean–vegetation model, which indicates a strong sensitivity of the model in that region.

c. Interannual variability of vegetation distribution

The interannual variability of the simulated radiative fractions is similar in magnitude in both models. The slightly higher values with LMDz–ORCHIDEE (Fig. 2) are partly due to the fire parameterization, not included in IBIS. The standard deviation is, for both models, less for trees than for grasses, and less for evergreen trees than for deciduous ones. In most regions it is below 5% for trees and it can reach 10%–20% for grasses. These numbers compare favorably with the interannual variability of PFT fractions derived from the 1982–94 AVHRR dataset by DeFries et al. (2000, their Fig. 6). In locations with no anthropogenic land cover changes, the woody vegetation has a standard deviation of less than 10%. For grasses and shrubs it ranges from 7% to 13%.

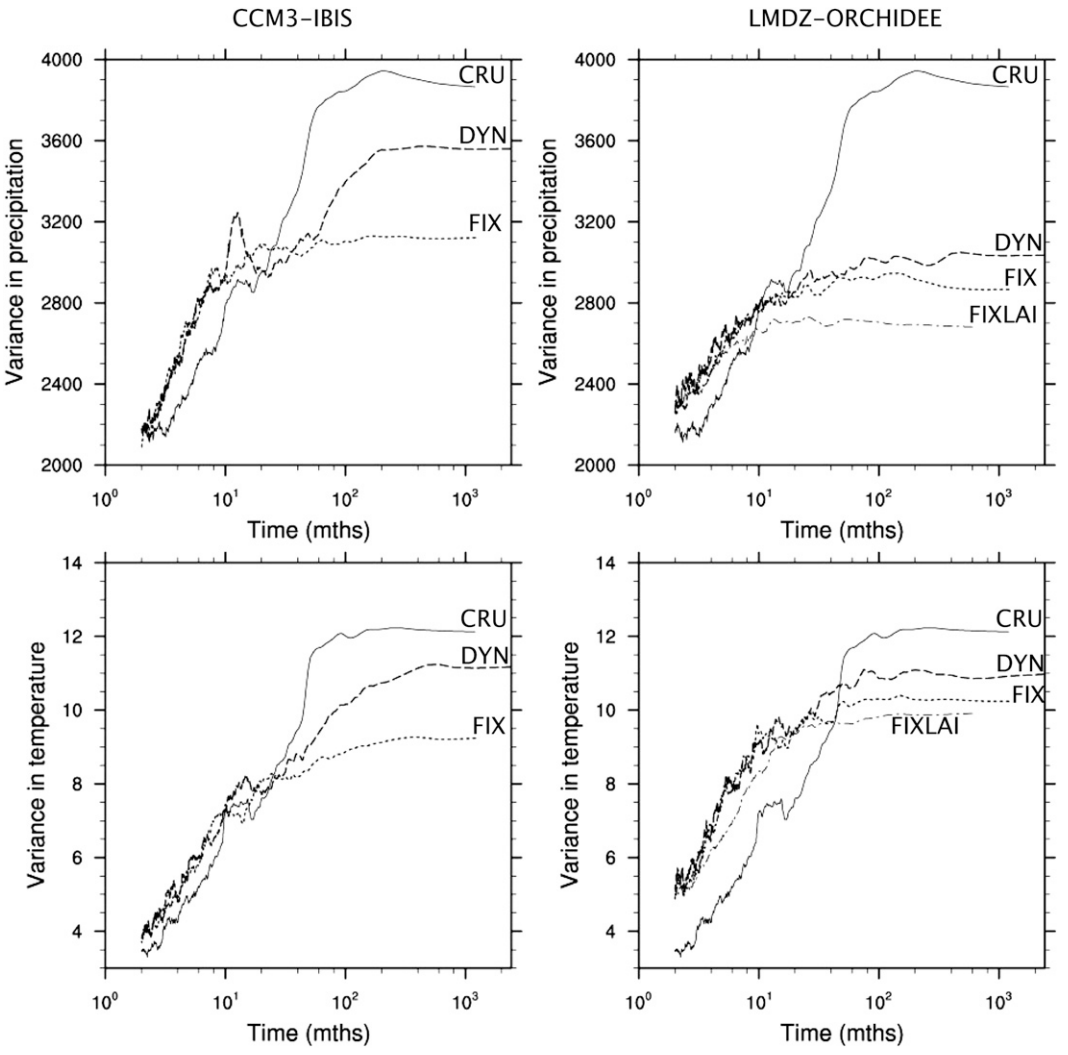

FIG. 3. Power spectra of the precipitation and temperature area averaged over land. (left) Results simulated by CCM3–IBIS with DYN and with FIX compared to the CRU dataset (New et al. 2000). (right) Results simulated by LMDz–ORCHIDEE with DYN, with FIX, and with FixLAI compared to the CRU dataset.

This interannual variability encompasses changes in both the amplitude and the seasonal cycle of the leaf area index for individual PFTs and in the changes in PFT composition. The higher interannual variability of grasses is due to their fast response time. Forest succession occurs at longer time scales, which reduces the interannual variability of tree PFTs.

5. Effects of vegetation dynamics on long-term climate variability

a. Spectral analysis

We calculated the power spectra of the monthly precipitation and reference height temperature simulated by the two models (Fig. 3). We first removed the average seasonal cycle and computed the area average of the local land spectra for the DYN and FIX experiments. As a reference, we plotted the power spectrum of observed precipitation and temperature from the Climate Research Unit (CRU) dataset (New et al. 2000), which covers 1901–98. The dataset was linearly detrended and resampled to the horizontal spatial resolution of the models. Temperature and precipitation from the CRU dataset include the feedback from the ocean and the vegetation over the twentieth century. As such, they are not directly comparable with our model results, which were obtained with fixed SSTs for the preindustrial period and do not include the interannual variability of the ocean. Hence, we expect the variability of our model results to be weaker than the CRU data at long time scales and stronger at short time scales. The ocean acts

as a long-term reservoir, dampening fast variations in the atmosphere and favoring long-term ones (see, e.g., Ghil 2002). As expected, both models, with and without vegetation dynamics, tend to underestimate the variability of temperature and precipitation at time scales longer than about 20 months (40 months for temperatures with LMDz) and overestimate the variability at smaller time scales.

When comparing the DYN and FIX simulations, the two models simulate an increase in the variability of precipitation and temperature at time scales larger than about 2 yr. This is in agreement with previous work (Delire et al. 2004; Wang et al. 2004), and confirms that changes in vegetation cover enhance the low-frequency variability of the atmosphere by adding a memory to the climate system. However, the increase in variance is much larger with CCM3–IBIS than with LMDz–ORCHIDEE. This partly results from the way the "fixed vegetation" module works in both models: the amplitude of the annual cycle of the LAI varies from year to year with LMDz–ORCHIDEE and is fixed with CCM3–IBIS (section 3, Table 1). The fractional cover of vegetation is the only thing that remains fixed in the FIX case with LMDz–ORCHIDEE. This allows for more feedbacks at interannual time scales between the vegetation and the atmosphere and a higher variance of the FIX case than with CCM3–IBIS. As a result, the difference between the power spectra of the DYN and FIX cases with LMDz–ORCHIDEE is smaller than with CCM3–IBIS.

As a test, we use an existing preindustrial simulation of LMDz–ORCHIDEE at the same resolution in which the LAI is fixed monthly (Fig. 3, the FixLAI curve). In FixLAI, there is no interannual variability in LAI at all. As expected, the difference in variance between the DYN and FixLAI modes is larger and more comparable to the one obtained with CCM3–IBIS, especially for precipitation. These results indicate that a large part of the vegetation dynamics is already included in the seasonal and interannual cycles of leaves. Therefore, letting the models calculate this variable is already a step toward a more realistic representation of the interactions between land and atmosphere.

The peak around 1 yr in the variance of the precipitation and, to a lesser extent temperature, simulated by CCM3–IBIS results from the dynamic vegetation module being called once a year in IBIS (Table 1). During the course of the year the plants assimilate carbon into the model but the fractional coverage of each PFT remains constant. At the end of each year, the carbon balance of each PFT is used to predict its fractional coverage and its peak LAI for the following year. This imposed annual change creates an unrealistic feedback to the atmosphere and the resulting peak in the precipitation variance. ORCHIDEE on the other hand calls its vegetation dynamics module once a day, and it is forced with a smoothed annual cycle of all forcing variables. This results in a smoother transition from year to year and the power spectrum in the DYN case does not present an annual peak.

b. Mechanisms enhancing the long-term variability

Delire et al. (2004) showed with CCM3–IBIS that feedback mechanisms between the vegetation and the atmosphere could explain the increased long-term variability of the atmosphere. The regions with persistent precipitation anomalies (hence increased long-term variability) correspond to transition zones between different ecosystems, like the Sahel. These regions present long-term variability in peak LAI and high correlation between the peak LAI of 1 yr and the precipitation of the subsequent year. Precipitation anomalies trigger long-term responses in the vegetation that feed back to the climate through biophysical processes. Changes in LAI that happen at short and long time scales affect the physical characteristics of the land surface such as albedo, roughness, soil moisture content, and evapotranspiration rates. Because these characteristics affect the energy and water fluxes toward the atmosphere above, and because they change at short and long time scales following LAI, they introduce long-term variability into the atmosphere (precipitation as shown in Delire et al. (2004) and temperature as shown here).

The mechanisms are the same with LMDz–ORCHIDEE. Rogard (2009) performed offline runs with the ORCHIDEE dynamic global vegetation model (DGVM) forced by climate data to analyze how vegetation dynamics affect the persistence of soil moisture anomalies. Wet and dry initial soil moisture conditions were imposed and the model was run in DYN and FIX modes over the Amazon basin and the Sahel. In each case (wet and dry, Amazon and Sahel), the initial soil moisture anomaly persists longer when vegetation dynamics are included. This enhanced soil moisture memory is due to slow changes in vegetation cover in response to the initial soil moisture anomaly. These slow changes modify the water and energy fluxes from the surface to the atmosphere and feed back to the soil moisture.

6. Are the simulated vegetation–atmosphere feedbacks of reasonable magnitude?

Having confirmed that vegetation dynamics do enhance the long-term variability of both temperature and precipitation in our two models, we now investigate the realism of this modeled response. Unrealistic feedbacks (by one or more order of magnitude) between the vegetation and the atmosphere would cast a doubt on the

validity of this conclusion. Although it is difficult from the observations in the atmospheric record to separate the respective impacts of vegetation and of ocean feedbacks, Frankignoul et al. (1998) developed a methodology for quantifying the feedback of the ocean to the atmosphere. Liu et al. (2006, hereafter L06) and Notaro et al. (2006) have adapted this method to assess the strength of the feedback from the vegetation to the atmosphere from the observations. L06 propose a parameter λ that gives a measure of the feedback efficiency of the vegetation on the atmosphere. Here, λ is given by the lagged covariance between a slow vegetation variable $V(t)$ and a fast atmospheric variable $A(t)$, assuming vegetation leads the atmosphere, divided by the lagged autocovariance of the vegetation variable $V(t)$:

$$\lambda = \frac{\langle V(t-\tau), A(t)\rangle}{\langle V(t-\tau), V(t)\rangle}, \quad \text{for} \quad \tau > 0,$$

where the angle brackets denote the covariance, t is time, and τ is the lag. The feedback parameter is computed as the weighted average from the first three lags (weights of 1.0, 0.5, and 0.25 for lags of 1, 2, and 3 months, respectively). The fraction of explained variance is computed as the variance of the part of the atmospheric signal that responds to a change in vegetation $\lambda V(t)$ divided by the variance of the whole atmospheric signal:

$$\frac{\sigma^2[\lambda V(t)]}{\sigma^2[A(t)]},$$

where σ^2 denotes the variance. As a proxy for vegetation activity, L06 chose the fraction of photosynthetically active radiation (FPAR) derived from the NDVI.

We applied this method to our simulations and qualitatively compared our results to the ones derived from the observations of L06. Quantitative comparison is more difficult because 1) our protocol simulates the preindustrial period with fixed climatological SSTs and natural vegetation, while L06 analyzed the end of the twentieth century and included both climate and land-use changes, and 2) there are few statistically significant regions in the observations due to the shortness of the NDVI dataset. In ORCHIDEE, FPAR is calculated as the foliage projected cover (section 4). This often-used approximation neglects the vegetation albedo. FPAR is calculated by the radiation code in IBIS but was not saved. We then used the foliage projected cover as in ORCHIDEE.

a. Feedback on temperature and explained variance

Both of the models used in this study simulate a positive feedback parameter of vegetation on temperature in the mid- to high latitudes (Figs. 4 and 5), in agreement with L06 (Fig. 12 of their paper). Most values range from 0.05° to 2°C$(0.1\text{FPAR})^{-1}$ in absolute value. These positive values result from the well-known snow–albedo feedback documented in observations (see, e.g., Chapin et al. 2005) and simulations [see, e.g., Snyder et al. (2004a), Strengers et al. (2010), or Bonan (2002) and Foley et al. (2003) for a review]. When vegetation cover increases (especially trees and shrubs), it partially masks the snow on the ground. The albedo is reduced, and the amount of solar energy reflected to space decreases (mostly in fall and spring). As a result, the available energy and surface temperature increase, thereby favoring the growth of vegetation. Negative values of the feedback parameter are simulated as well as observed in semiarid regions like the Sahel, the Middle East, the North American southwest, and parts of Australia. The feedback is smaller in absolute value [less than 1°C $(0.1\ \text{FPAR})^{-1}$] than the observed and simulated values in the high latitudes. This negative feedback involves transpiration. When vegetation cover increases in semiarid regions, transpiration tends to increase, cooling the surface directly through the release of latent heat, and indirectly by humidifying the atmosphere and favoring convection. Grasses and shrubs are the main PFTs in these negative feedback regions [spatial correlation between the mean FPC of grasses and the feedback parameter between 60°S and 40°N equals −0.5 with CCM3–IBIS and −0.4 with LMDz–ORCHIDEE).

There is a greater discrepancy between the models over the equatorial regions. The LMDz–ORCHIDEE model almost consistently simulates a negative feedback of the vegetation on surface temperature, except in the evergreen forests of central Africa, while in CCM3–IBIS positive feedbacks are simulated in large regions of Africa, South America, and the Indonesian Archipelago. In that respect CCM3–IBIS behaves more like the observations, although as mentioned by L06, there are few statistically significant zones in the equatorial regions. This observed positive feedback in the equatorial regions has not been explained yet. With CCM3–IBIS, the positive feedback is due to the behavior of the canopy radiation transfer scheme when LAI is greater than six. Contrary to what happens when LAI is less than six, the radiation code simulates a small increase (~0.001) in albedo for a small increase (~0.2) in LAI. Because incoming solar radiation is great in this region, this very small increase in albedo results in a decrease in net radiation that is sufficient to increase the monthly average surface air temperature by 0.1°C through decreased latent cooling. Tropical evergreen and to a lesser extent drought deciduous forests are located in the regions with these positive feedbacks in the observations, with CCM3–IBIS and in Africa with LMDz–ORCHIDEE.

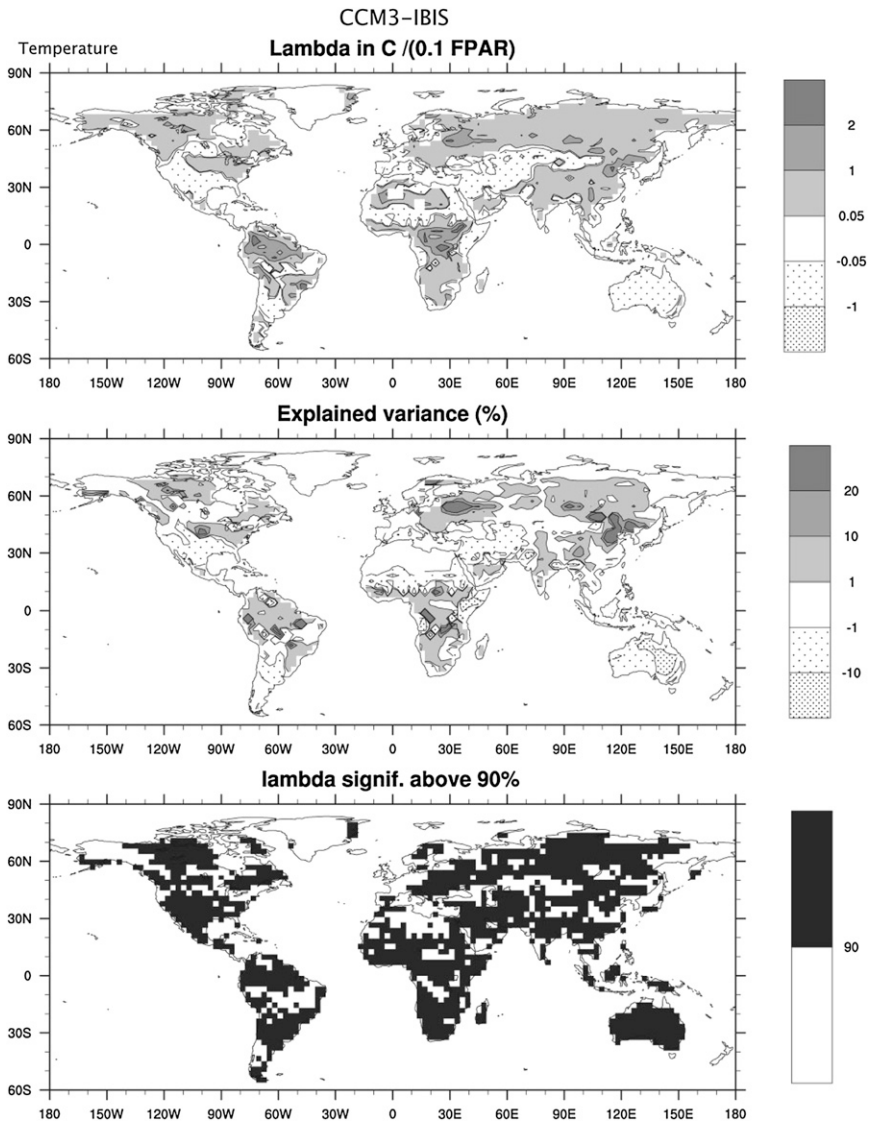

FIG. 4. (top) The vegetation feedback parameter, (middle) percent of monthly temperature variance explained (in the statistical sense) by the vegetation–temperature feedback, and (bottom) regions that are statistically significant over 90% using a Monte Carlo bootstrap technique for monthly temperature anomalies simulated by CCM3–IBIS. Regions with very small autocorrelations of vegetation are masked out.

The negative feedback from LMDz–ORCHIDEE can partly be explained by the anomalous dry conditions simulated in the equatorial regions (section 4a). The vegetation (mainly grasses; Fig. 1) is seasonally water limited. Seasonal and interannual changes in latent heat flux are larger than in humid tropical regions and impact the surface temperature, as they do in semiarid regions. Conversely, the positive feedback simulated by CCM3–IBIS over the Arabian Peninsula or southern Africa is due to the wet bias of the model in these regions (section 4a).

The feedback-induced variance $\sigma^2[\lambda_T V(t)]$ calculated by L06 explains (in the statistical sense) over 20% of the total observed temperature variance in large areas of the mid- to high latitudes of the Northern Hemisphere. In the rest of the world, the feedback-induced variance does not exceed 10% of the variance. Model-explained variances are smaller, especially in the high latitudes. They range from 1% to 10% of the total temperature variance in most regions of the world. The value of 20% is only reached in some isolated regions instead of the large areas located around the Arctic as observed. This is the result of the exaggerated interannual variability simulated by both models in the Arctic regions (not shown), and can be attributed in part to the lack of oceanic and

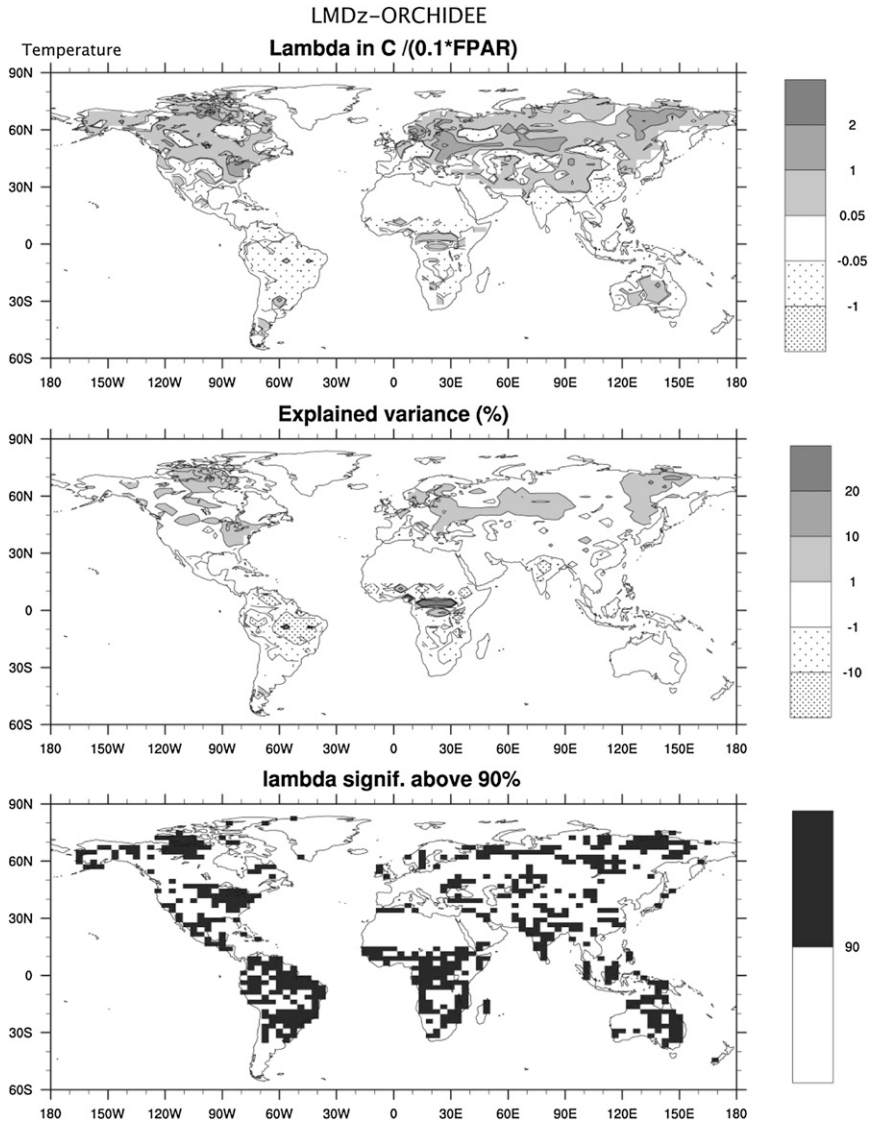

FIG. 5. As in Fig. 4, but for monthly temperature anomalies simulated by LMDz–ORCHIDEE.

sea ice feedbacks. Indeed, oceanic feedbacks tend to dampen variability at interannual time scales while increasing variability at longer time scales (e.g., Ghil 2002).

b. Feedback on precipitation and explained variance

The feedback of vegetation on precipitation is much more difficult to interpret in the data (L06). There are very few statistically significant regions and the areas with positive and negative feedback parameters cannot be easily linked to a particular latitude band, climate regime, or vegetation type. An exception seems to be the grasslands and shrublands of northeast Brazil, eastern Africa, eastern Asia, the U.S. Great Plains, northern Australia, and parts of central Europe, which are linked to weak positive feedbacks from the vegetation to the atmosphere in the dataset.

Both models simulate a weak positive feedback over most land areas (Figs. 6 and 7) in disagreement with the observations. There are few and, in the case of LMDz–ORCHIDEE, extremely isolated exceptions to this positive feedback. CCM3–IBIS simulates some negative feedback regions in the Amazon Basin, the Congo Basin, Indonesia and eastern China, and northeast Siberia. The mostly positive feedback can be fairly easily explained in the models, especially in semiarid areas. As the vegetation foliage and cover increase, so does transpiration. Increased vegetation cover and foliage result in decreased

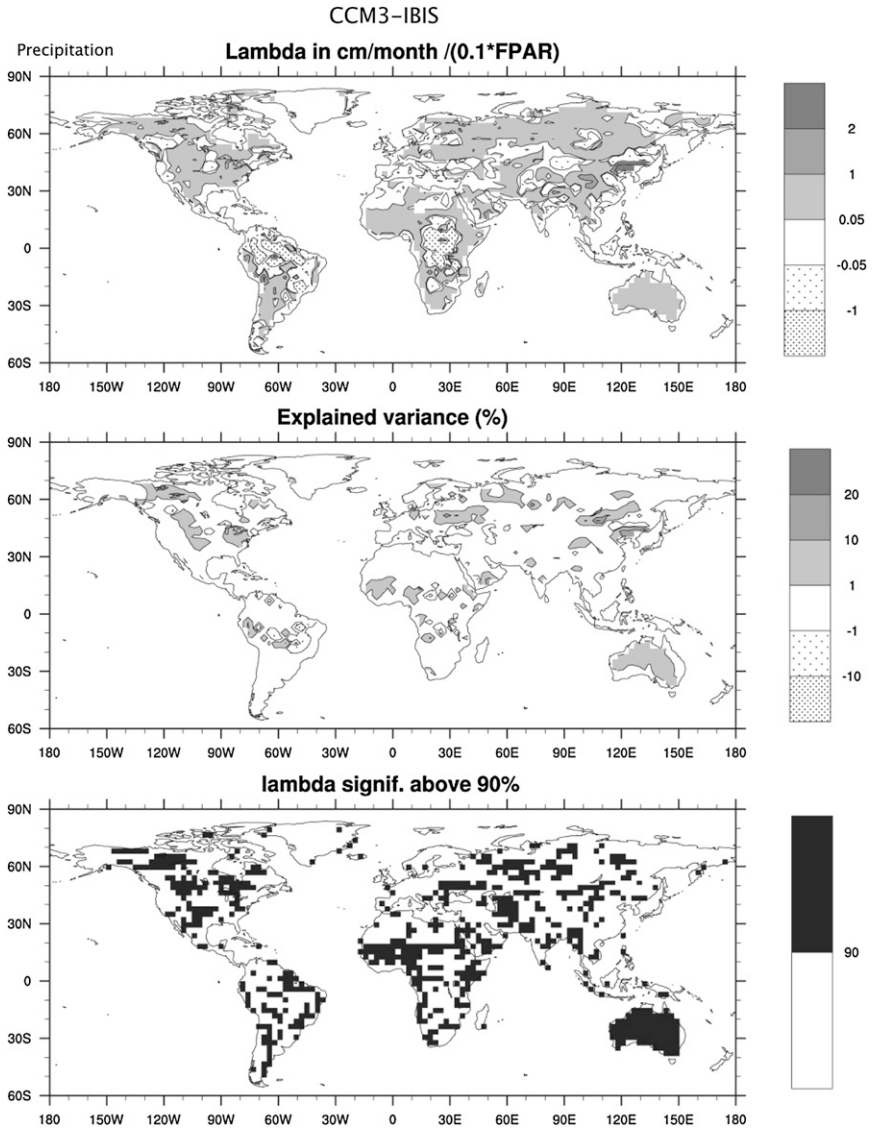

FIG. 6. As in Fig. 4, but for monthly precipitation anomalies simulated by CCM3–IBIS.

albedo and the available energy is also increased. With more energy, and more latent heat flux, convection is favored. This positive feedback linking increased fractional cover by vegetation to decreased albedo and increased transpiration has been largely reported upon in modeling studies, starting with Charney's hypothesis. In the high latitudes, the same chain of processes happens but the effects on transpiration are restricted to the growing season. During the rest of the year, the increase in albedo due to the above-mentioned snow–albedo feedback pattern plays the major role and acts mostly on temperature [see Snyder et al. (2004b) for a detailed description of the feedbacks in the different climates].

The percentage of precipitation variance explained by the vegetation feedback is very small in most regions of the world for both models. This is mostly due to the high variance of the monthly precipitation. The regions were it is higher than 1% tend to coincide with the regions of increased persistence of precipitation anomalies identified in Delire et al. 2004. They also correspond with the regions of intense atmosphere and land surface coupling identified by Koster et al. (2002) and the regions that experienced abrupt changes in rainfall during the twentieth century as diagnosed by Narisma et al. (2007).

c. Influence of scale on the vegetation feedback

L06 found that the intensity of the feedback and the fraction of explained variance tend to increase with increasing spatial and temporal scales. The global mean of the feedback efficiency on temperature and on precipitation

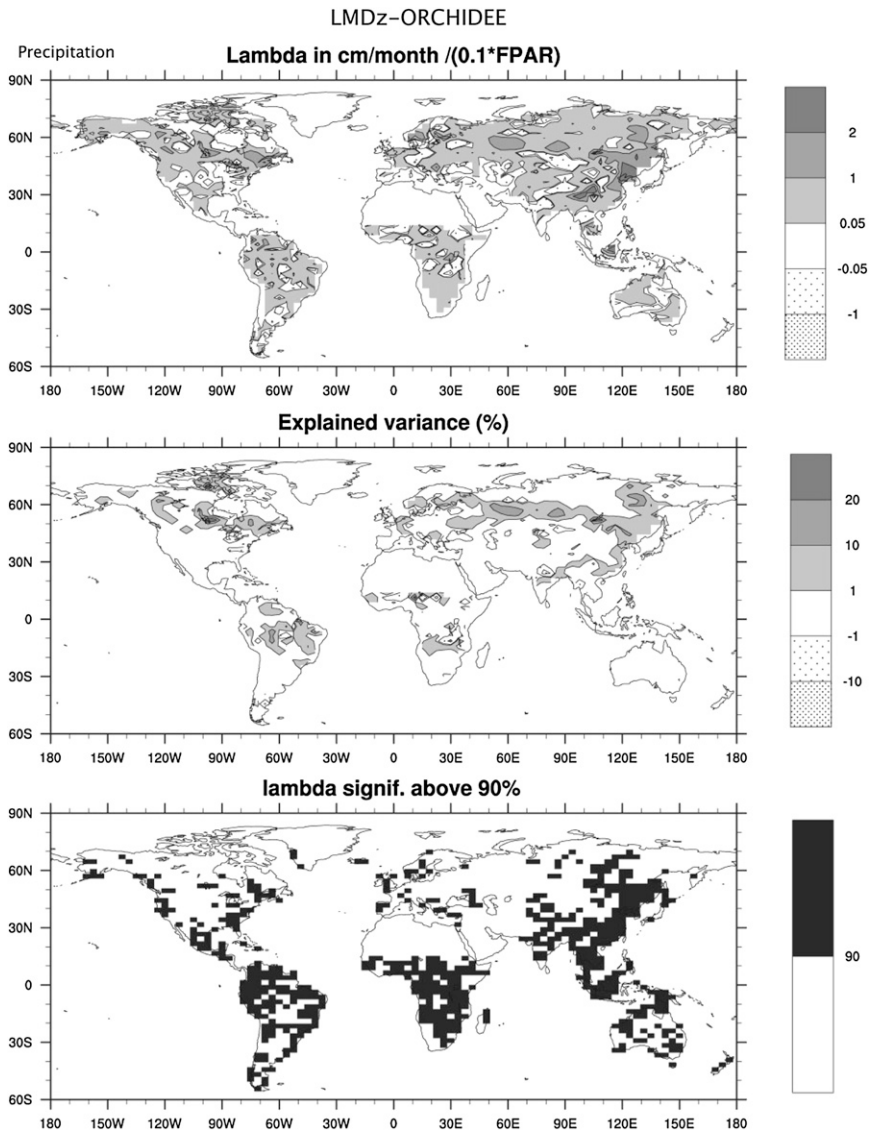

FIG. 7. As in Fig. 4, but for monthly precipitation anomalies simulated by LMDz–ORCHIDEE.

more than doubles when going from monthly to yearly data. Although changes in phenology happen at the seasonal time scale, competition between plant types resulting in succession is a slower process happening at time scales of a few years to several decades. The effects of the slower processes might be overshadowed by the fast ones when looking only at monthly results. The increase in explained variance is even more dramatic, from about 2% to ~40% when going from monthly to yearly data. As mentioned by L06 though, these results are largely speculative due to the shortness of the satellite record.

This is not an issue with the models. In agreement with the observations, the global land average of the feedback efficiency and the fraction of explained variance are larger with yearly rather than monthly data for both models (Table 2). The increase in feedback efficiency ranges from 25% to 150% (columns 1 and 3). The increase in the fraction of the vegetation feedback explained variance is even more pronounced, with a fourfold increase for the vegetation–temperature feedback and a 10–20-fold increase for the vegetation–precipitation feedback (columns 2 and 4). In the case of precipitation, the large increase in the fraction of feedback explained the variance is mostly due to the much smaller variance of the precipitation at yearly compared to monthly time scales. The overall geographic distribution of the feedback efficiency is similar to that deduced from monthly data with both models for both temperature and precipitation (not shown).

TABLE 2. Global land average of the vegetation feedback efficiency (in absolute values) and magnitude of the feedback-explained variances simulated by CCM3–IBIS and LMDz–ORCHIDEE. Units are in °C.$(0.1\ \mathrm{FPAR})^{-1}$ for the vegetation–temperature feedback and cm month^{-1} $(0.1\ \mathrm{FPAR})^{-1}$ for the vegetation–precipitation feedback. The results are given for monthly and yearly binned data.

	$\lvert\lambda_T\rvert$	$\sigma^2(\lvert\lambda_T \mathrm{FPAR}\rvert)/\sigma^2(T)$	$\lvert\lambda_P\rvert$	$\sigma^2(\lvert\lambda_P \mathrm{FPAR}\rvert)/\sigma^2(P)$
CCM3–IBIS	0.4/0.5	5/21	0.4/0.6	1/9
LMDz–ORCHIDEE	0.3/0.4	5/22	0.4/1.0	1/24

d. Discussion

The fairly realistic feedback parameters in large regions of the globe (same order of magnitude as the observations) support our hypothesis that vegetation dynamics may enhance climate variability. Our conclusions differ from those of Crucifix et al. (2005), who found a very weak impact of vegetation dynamics on climate variability in their HadSM3 simulations. Several explanations are possible. Among other things, HadSM3 is coupled to a ''slab ocean'' with prescribed spatially and seasonally varying heat fluxes while we have imposed fixed climatological SSTs. The use of a slab ocean could affect the variability of the atmosphere and overshadow the effects of vegetation. More importantly, as suggested by Crucifix et al. (2005) and confirmed by Koster et al. (2002, 2006) HadSM3 has a fairly weak coupling strength between the land surface and the atmosphere compared to other models. A similar change in land surface conditions (soil moisture in the Koster et al. studies) has a weaker impact on the atmosphere with HAdSM3 than with other models. This weak soil moisture–atmosphere feedback most likely translates into weak vegetation–atmosphere feedbacks since soil moisture and vegetation affect the atmosphere through similar feedback processes. A feedback analysis of Crucifix et al.'s (2005) simulations might have shown weaker than observed feedbacks, confirming the weak land surface–atmosphere coupling strength hypothesis.

7. Summary and conclusions

In this paper we compared how two different coupled climate–vegetation models simulate the effects of vegetation dynamics on climate variability. We performed two sets of simulations of the preindustrial climate with both coupled climate–vegetation models, using fixed climatological sea surface temperatures: one set taking into account vegetation cover dynamics and the other keeping the vegetation cover fixed.

To cite just a few differences between the models, CCM3 is a spectral model while LMDz is a Cartesian grid based model, and the vegetation cover with IBIS is represented by a homogeneous mix of several PFTs in two canopies over the whole grid cell while ORCHIDEE represents a mosaic of PFTs as a single canopy layer in separate tiles. The mean climate and vegetation simulated by the two models for the preindustrial period are quite different in some regions of the world. Overall, LMDz–ORCHIDEE tends to simulate more forests in the northern high latitudes while CCM3–IBIS tends to simulate more forests in the tropics.

Despite these differences between the mean climate and vegetation, our spectral analysis of the precipitation and temperature fields over land shows that for both models vegetation dynamics enhance the low-frequency variability of the biosphere–atmosphere system at time scales from a few years to a century. This is in agreement with our previous results (Delire et al. 2004) and with the results of Wang et al. (2004), and confirms that vegetation dynamics introduce a long-term memory into the climate system by slowly modifying the physical characteristics of the land surface (albedo, evapotranspiration, roughness). With LMDz–ORCHIDEE we also showed that the seasonal and interannual cycles of leaves alone enhance the variability of the system. Letting the models calculate this variable but keeping the vegetation cover fixed, as is done in most IPCC coupled climate models, is therefore a step toward a realistic representation of the interactions between land and atmosphere.

To evaluate the realism of these simulated feedback processes in our models, we used Liu et al.'s (2006) approach to statistically estimate the efficiency of the vegetation feedback on the temperature and precipitation for both models and compared them to the feedback calculated from observations. Our analysis shows that the models simulate feedbacks of the right signs and orders of magnitude over large regions of the globe at monthly time scales: positive feedback on temperature in the mid- to high latitudes, negative feedback in semiarid regions, and positive feedback on precipitation in semiarid regions. The models tend to underestimate the fraction of variance of the temperature and precipitation explained by the vegetation feedback, especially in the Arctic. As with the observations, the fraction of variance explained by the vegetation feedback increases with the temporal scale. This is also true to a lesser extent for the feedback efficiency itself. Most of the disagreement between models and between the models and the observations occurs in

the tropics where oceans play a dominant role in climate variability. Alessandri and Navarra (2008) showed for instance that the component of rainfall variability that is forced by vegetation is dominated by an oscillation related to ENSO. Our chosen experimental setup (fixed SSTs) might explain the poor agreement between the model and the observations in the tropics.

The statistical feedback analysis has several limitations. Among others, first, we cannot test the realism of the simulated feedbacks at decadal to century time scales due to the shortness of the FPAR time series. Second, Liu et al.'s (2006) method is based on linear statistics and does not adequately represent nonlinear feedback processes. Despite these caveats, this feedback efficiency analysis shows that the coupled models simulate the biophysical interactions reasonably well at time scales of up to a few years.

We did not include managed ecosystems in our study of the preindustrial period. Pasture and agriculture are likely to affect the variability of the climate, especially during the twentieth and twenty-first centuries (Wang and Eltahir 2000b; Cook et al. 2009). Many other processes affecting the functioning of terrestrial ecosystems are not represented in these models and could modulate the variability of the climate–biosphere system. Some processes (like PFT competition) are also represented in fairly coarse ways. We did not include the biogeochemical interactions between vegetation and the atmosphere. The exchange of CO_2 between the land and the atmosphere through photosynthesis and respiration, for instance, is bound to affect climate variability by directly changing the radiative balance of the atmosphere but also by affecting the competition between species. To isolate the effects of vegetation dynamics, we imposed fixed sea surface temperatures, thereby preventing any interaction with the oceans known to influence climate variability from interannual to centennial time scales.

Despite these caveats, we confirmed by using two very different models that terrestrial ecosystems may play an important role in enhancing the long-term variability of the climate system. Terrestrial ecosystems provide a ''memory'' to the climate system, causing important variations in the climate and ecological conditions on long time scales.

Acknowledgments. This work was supported by the French Agence Nationale de la Recherche's (ANR) ''programme blanc'' under Contract ANR-05-BLAN-0167. The computing was done at the French Commissariat à l'Energie Atomique (CEA) and at the European Centre for Medium-Range Weather Forecasts (ECMWF), which we wish to thank. The authors are very grateful to Erwan Rogard who carried out part of the offline analysis used here during his master's thesis. We thank Bertrand Decharme for motivating discussions, Michael Coe for a careful reading of the manuscript, and three anonymous reviewers who helped improve this manuscript. We are also grateful to the developers of the free NCL software used for the figures.

REFERENCES

Alessandri, A., and A. Navarra, 2008: On the coupling between vegetation and rainfall inter-annual anomalies: Possible contributions to seasonal rainfall predictability over land areas. *Geophys. Res. Lett.,* **35,** L02718, doi:10.1029/2007GL032415.

Amthor, J. S., 1984: The role of maintenance respiration in plant growth. *Plant Cell Environ,* **7,** 561–569.

Ball, J. T., I. E. Woodrow, and J. A. Berry, 1987: A model predicting stomatal conductance and its contribution to the control of photosynthesis under different environmental conditions. *Progress in Photosynthesis Research*, J. Biggins, Ed., Vol. IV, Martinus Nijhohf, 221–224.

Bonan, G. B., 1997: Effects of land use on the climate of the United States. *Climatic Change,* **37,** 449–486.

——, 1999: Frost followed the plow: Impacts of deforestation on the climate of the United States. *Ecol. Appl.,* **9,** 1305–1315.

——, 2002: *Ecological Climatology: Concepts and Applications*. Cambridge University Press, 550 pp.

——, D. Pollard, and S. L. Thompson, 1992: Effects of boreal forest vegetation on global climate. *Nature,* **359,** 716–718.

——, F. S. Chapin III, and S. L. Thompson, 1995: Boreal forest and tundra ecosystems as components of the climate system. *Climatic Change,* **29,** 145–167.

Botta, A., N. Viovy, P. Ciais, P. Friedlingstein, and P. Monfray, 2000: A global prognostic scheme of leaf onset using satellite data. *Global Change Biol.,* **6,** 709–725.

Bounoua, L., R. DeFries, G. J. Collatz, P. Sellers, and H. Khan, 2002: Effects of land cover conversion on surface climate. *Climatic Change,* **52,** 29–64.

Brovkin, V., M. Claussen, V. Petoukhov, and A. Ganopolski, 1998: On the stability of the atmosphere–vegetation system in Sahara/Sahel region. *J. Geophys. Res.,* **103,** 31 613–31 624.

Chapin, F. S., and Coauthors, 2005: Role of land-surface changes in Arctic summer warming. *Science,* **310,** 657–660.

Charney, J. G., P. H. Stone, and W. J. Quirk, 1975: Drought in the Sahara: A biogeophysical feedback mechanism. *Science,* **187,** 434–435.

——, W. J. Quirk, S.-H. Chow, and J. Kornfield, 1977: A comparative study of the effects of albedo change on drought in semiarid regions. *J. Atmos. Sci.,* **34,** 1366–1385.

Chase, T. N., R. A. Pielke Sr., T. G. F. Kittel, R. R. Nemani, and S. W. Running, 2000: Simulated impacts of historical land cover changes on global climate in northern winter. *Climate Dyn.,* **16,** 93–105.

Ciais, P., and Coauthors, 2005: Europe-wide reduction in primary productivity caused by heat and drought in 2003. *Nature,* **437,** 529–533.

Coe, M. T., M. H. Costa, A. Botta, and C. M. Birkett, 2002: Long-term simulations of discharge and floods in the Amazon basin. *J. Geophys. Res.,* **107,** 8044, doi:10.1029/2001JD000740.

——, ——, and B. S. Soares-Filhoc, 2009: The influence of historical and potential future deforestation on the stream flow of the Amazon River—Land surface processes and atmospheric feedbacks. *J. Hydrol.,* **369,** 165–174.

Collatz, G. J., J. T. Ball, C. Grivet, and J. A. Berry, 1991: Physiological and environmental regulation of stomatal conductance, photosynthesis and transpiration—A model that includes a laminar boundary-layer. *Agric. For. Meteor.,* **54,** 107–136.

——, M. Ribas-Carbo, and J. A. Berry, 1992: Coupled photosynthesis-stomatal conductance model for leaves of C4 plants. *Aust. J. Plant Physiol.,* **19,** 519–538.

Cook, B. I., R. L. Miller, and R. Seager, 2009: Amplification of the North American "Dust Bowl" drought through human induced land degradation. *Proc. Natl. Acad. Sci. USA,* **106,** 4997–5001.

Costa, M. H., and J. A. Foley, 1997: Water balance of the Amazon Basin: Dependence on vegetation cover and canopy conductance. *J. Geophys. Res.,* **102** (D20), 23 973–23 989.

——, S. N. M. Yanagi, P. J. O. P. Souza, A. Ribeiro, and E. J. P. Rocha, 2007: Climate change in Amazonia caused by soybean cropland expansion, as compared to caused by pastureland expansion. *Geophys. Res. Lett.,* **34,** L07706, doi:10.1029/2007GL029271.

Cox, P. M., R. A. Betts, C. D. Jones, S. A. Spall, and I. J. Totterdell, 2000: Acceleration of global warming due to carbon-cycle feedbacks in a coupled climate model. *Nature,* **408,** 750–750.

Crucifix, M., R. A. Betts, and P. M. Cox, 2005: Vegetation and climate variability: A GCM modelling study. *Climate Dyn.,* **24,** 457–467.

DeFries, R., M. Hansen, and J. Townshend, 2000: Global continuous fields of vegetation characteristics: A linear mixture model applied to multiyear 8km AVHRR data. *Int. J. Remote Sens.,* **21,** 1389–1414.

Delire, C., and J. Foley, 1999: Evaluating the performance of a land surface/ecosystem model with biophysical measurements from contrasting environments. *J. Geophys. Res.,* **104** (D14), 16 895–16 909.

——, S. Levis, G. Bonan, and J. A. Foley, 2002: Comparison of the climate simulated by the CCM3 using 2 different processed based land-surface/ecological models. *Climate Dyn.,* **19,** 657–669.

——, J. Foley, and S. Thompson, 2003: Evaluating the carbon cycle of a coupled atmosphere–biosphere. *Global Biogeochem. Cycles,* **17,** doi:10.1029/2002GB001870.

——, J. A. Foley, and S. Thompson, 2004: Long-term internal variability in a coupled atmosphere–biosphere model. *J. Climate,* **17,** 3947–3959.

de Noblet-Ducoudré, N., R. Claussen, and C. Prentice, 2000: Mid Holocene greening of the Sahara: First results of the GAIM 6000 year BP experiment with two asynchronously coupled atmosphere/biome models. *Climate Dyn.,* **16,** 643–659.

de Rosnay, P., and J. Polcher, 1998: Modelling root water uptake in a complex land surface scheme coupled to a GCM. *Hydrol. Earth Syst. Sci.,* **2,** 239–255.

Dickinson, R. E., and A. Henderson-Sellers, 1988: Modelling tropical deforestation: A study of GCM land-surface parameterizations. *Quart. J. Roy. Meteor. Soc.,* **114,** 439–462.

Dorman, J. L., and P. J. Sellers, 1989: A global climatology of albedo roughness length and stomatal resistance for atmospheric general circulation models as represented by the Simple Biosphere Model (SiB). *J. Appl. Meteor.,* **28,** 833–855.

Douville, H., and J.-F. Royer, 1997: Influence of the temperate and boreal forests on the Northern Hemisphere climate in the Météo-France climate model. *Climate Dyn.,* **13,** 57–74.

Ducoudré, N. I., K. Laval, and A. Perrier, 1993: SECHIBA, a new set of parameterizations of the hydrologic exchanges at the land–atmosphere interface within the LMD atmospheric general circulation model. *J. Climate,* **6,** 248–273.

Farquhar, G. D., S. von Caemmerer, and J. A. Berry, 1980: A biochemical model of photosynthetic CO_2 assimilation in leaves of C3 species. *Planta,* **149,** 78–90.

Foley, J. A., C. I. Prentice, N. Ramankutty, S. Levis, D. Pollard, S. Sitch, and A. Haxeltine, 1996: An integrated biosphere model of land surface processes, terrestrial carbon balance, and vegetation dynamics. *Global Biogeochem. Cycles,* **10,** 603–628.

——, M. Heil Costa, C. Delire, N. Ramankutty, and P. Synder, 2003: Green surprise? How the biosphere could affect the future of our climate. *Front. Ecol. Environ.,* **1,** 38–44.

Frankignoul, C., A. Czaja, and B. L'Heveder, 1998: Air–sea feedback in the North Atlantic and surface boundary conditions for ocean models. *J. Climate,* **11,** 2310–2324.

Ghil, M., 2002: Natural climate variability. *Encyclopedia of Global and Environmental Change,* T. Munn, Ed., John Wiley and Sons, 544–549.

Givnish, T. J., 2002: Adaptive significance of evergreen vs. deciduous leaves: Solving the triple paradox. *Silva Fenn.,* **36,** 703–743.

Hahmann, A. N., and R. E. Dickinson, 1997: RCCM2–BATS model over tropical South America: Applications to tropical deforestation. *J. Climate,* **10,** 1944–1964.

Hourdin, F., and Coauthors, 2006: The LMDZ4 general circulation model: Climate performance and sensitivity to parameterized physics with emphasis on tropical convection. *Climate Dyn.,* **27,** 787–813.

Kiehl, J. T., J. J. Hack, G. B. Bonan, B. A. Boville, D. L. Williamson, and P. J. Rasch, 1998: The National Center for Atmospheric Research Community Climate Model: CCM3. *J. Climate,* **11,** 1131–1149.

Koster, R. D., P. A. Dirmeyer, A. N. Hahmann, R. Ijpelaar, L. Tyahla, P. Cox, and M. J. Suarez, 2002: Comparing the degree of land–atmosphere interaction in four atmospheric general circulation models. *J. Hydrometeor.,* **3,** 363–375.

——, and Coauthors, 2006: GLACE: The Global Land–Atmosphere Coupling Experiment. Part I: Overview. *J. Hydrometeor.,* **7,** 590–610.

Krinner, G., and Coauthors, 2005: A dynamic global vegetation model for studies of the coupled atmosphere–biosphere system. *Global Biogeochem. Cycles,* **19,** 1–33.

Kucharik, C. J., and Coauthors, 2000: Testing the performance of a dynamic global ecosystem model: Water balance, carbon balance, and vegetation structure. *Global Biogeochem. Cycles,* **14,** 795–825.

——, K. R. Brye, J. M. Norman, J. A. Foley, S. T. Gower, and L. G. Bundy, 2001: Measurements and modeling of carbon and nitrogen cycling in agroecosystems of southern Wisconsin: Potential for SOC sequestration during the next 50 years. *Ecosystems (N. Y.),* **4,** 237–258.

——, C. Barford, M. El Maayar, S. C. Wofsy, R. K. Monson, and D. D. Baldocchi, 2006: A multiyear evaluation of a dynamic global vegetation model at three AmeriFlux forest sites: Vegetation structure, phenology, soil temperature, and CO_2 and H_2O vapor exchange. *Ecol. Modell.,* **196,** 1–31.

Kutzbach, J. E., G. Bonan, J. Foley, and S. P. Harrison, 1996: Vegetation and soil feedbacks on the response of the African monsoon to orbital forcing in the early to middle Holocene. *Nature,* **384,** 623–626.

Lean, J., and D. A. Warrilow, 1989: Simulation of the regional climatic impact of Amazon deforestation. *Nature,* **342,** 411–413.

Lenters, J. D., M. T. Coe, and J. A. Foley, 2000: Surface water balance of the continental United States, 1963–1995: Regional

evaluation of a terrestrial biosphere model and the NCEP/NCAR reanalysis. *J. Geophys. Res.,* **105** (D17), 22 393–22 425.

Levis, S., J. A. Foley, V. Brovkin, and D. Pollard, 1999: On the stability of the high-latitude climate–vegetation system in a coupled atmosphere–biosphere model. *Global Ecol. Biogeogr.,* **8,** 489–500.

——, ——, and D. Pollard, 2000: Large-scale vegetation feedbacks on a doubled CO_2 climate. *J. Climate,* **13,** 1313–1325.

Liu, Z., M. Notaro, J. Kutzbach, and N. Liu, 2006: Assessing global vegetation–climate feedbacks from observations. *J. Climate,* **19,** 787–814.

Lotsch, A., M. A. Friedl, B. T. Anderson, and C. J. Tucker, 2003: Coupled vegetation–precipitation variability observed from satellite and climate records. *Geophys. Res. Lett.,* **30,** 1774, doi:10.1029/2003GL017506.

Marti, O., and Coauthors, 2010: Key features of the IPSL ocean atmosphere model and its sensitivity to atmospheric resolution. *Climate Dyn.,* **34,** 1–26, doi:10.1007/s00382-009-0640-6.

Morales, P., and Coauthors, 2005: Comparing and evaluating process-based ecosystem model predictions of carbon and water fluxes in major European forest biomes. *Global Change Biol.,* **11,** 2211–2233.

Narisma, G. T., J. A. Foley, R. Licker, and N. Ramankutty, 2007: Abrupt changes in rainfall during the twentieth century. *Geophys. Res. Lett.,* **34,** L06710, doi:10.1029/2006GL028628.

New, M., M. Hulme, and P. D. Jones, 2000: Representing twentieth-century space–time climate variability. Part II: Development of 1901–96 monthly grids of terrestrial surface climate. *J. Climate,* **13,** 2217–2238.

——, D. Lister, M. Hulme, and I. Makin, 2002: A high-resolution data set of surface climate over global land areas. *Climate Res.,* **21,** 1–25.

Ngo-Duc, T., K. Laval, J. Polcher, and A. Cazenave, 2005a: Contribution of continental water to sea level variations during the 1997–1998 El Niño–Southern Oscillation event: Comparison between Atmospheric Model Intercomparison Project simulations and TOPEX/Poseidon satellite data. *J. Geophys. Res.,* **110,** D09103, doi:10.1029/2004JD004940.

——, ——, ——, A. Lombard, and A. Cazenave, 2005b: Effects of land water storage on global mean sea level over the past half century. *Geophys. Res. Lett.,* **32,** L09704, doi:10.1029/2005GL022719.

Nicholson, S., 2000: Land surface processes and Sahel climate. *Rev. Geophys.,* **38,** 117–139.

Nobre, C. A., P. J. Sellers, and J. Shukla, 1991: Amazonian deforestation and regional climate change. *J. Climate,* **4,** 957–988.

Notaro, M., Z. Liu, and J. W. Williams, 2006: Observed vegetation–climate feedbacks in the United States. *J. Climate,* **19,** 763–786.

Piao, S. L., P. Friedlingstein, P. Ciais, L. M. Zhou, and A. P. Chen, 2006: Effect of climate and CO_2 changes on the greening of the Northern Hemisphere over the past two decades. *Geophys. Res. Lett.,* **33,** L23402, doi:10.1029/2006GL028205.

——, ——, ——, N. de Noblet-Ducoudre, D. Labat, and S. Zaehle, 2007: Changes in climate and land use have a larger direct impact than rising CO_2 on global river runoff trends. *Proc. Nat. Acad. Sci. USA,* **104,** 15 242–15 247.

Pielke, R. A., and Coauthors, 2002: The influence of land-use change and landscape dynamics on the climate system: Relevance to climate-change policy beyond the radiative effect of greenhouse gases. *Philos. Trans. Roy. Soc. London,* **360A,** 1705–1719.

Pitman, A. J., and Coauthors, 2009: Uncertainties in climate responses to past land cover change: First results from the LUCID intercomparison study. *Geophys. Res. Lett.,* **36,** L14814, doi:10.1029/2009GL039076.

Prentice, C., W. Cramer, S. P. Harrison, R. Leemans, R. A. Monserud, and A. M. Solomon, 1992: A global biome model based on plant physiology and dominance, soil properties and climate. *J. Biogeogr.,* **19,** 117–134.

Ramankutty, N., C. Delire, and P. Snyder, 2006: Feedbacks between agriculture and climate: An illustration of the potential unintended consequences of human land use activities. *Global Planet. Change,* **54,** 79–93.

Rayner, N. A., D. E. Parker, E. B. Horton, C. K. Folland, L. V. Alexander, D. P. Rowell, E. C. Kent, and A. Kaplan, 2003: Global analyses of sea surface temperature, sea ice, and night marine air temperature since the late nineteenth century. *J. Geophys. Res.,* **108,** 4407, doi:10.1029/2002JD002670.

Rogard, E., 2009: Évaluation de la capacité du système sol-plante du modèle ORCHIDEE à générer de la persistance d'évènements secs et pluvieux. M.S. thesis, University Paris Diderot (Paris 7), Paris, France, 82 pp.

Senna, M. C. A., M. H. Costa, and Y. E. Shimabukuro, 2005: Fraction of photosynthetically active radiation absorbed by Amazon tropical forest: A comparison of field measurements, modeling, and remote sensing. *J. Geophys. Res.,* **110,** G01008, doi:10.1029/2004JG000005.

——, ——, and G. F. Pires, 2009: Vegetation–atmosphere–soil nutrient feedbacks in the Amazon for different deforestation scenarios. *J. Geophys. Res.,* **114,** D04104, doi:10.1029/2008JD010401.

Sitch, S., and Coauthors, 2003: Evaluation of ecosystem dynamics, plant geography and terrestrial carbon cycling in the LPJ dynamic global vegetation model. *Global Change Biol.,* **9,** 161–185.

Snyder, P. K., C. Delire, and J. A. Foley, 2004a: Evaluating the influence of different vegetation biomes on the global climate. *Climate Dyn.,* **23,** 279–302.

——, J. A. Foley, M. H. Hitchman, and C. Delire, 2004b: Analyzing the effects of complete tropical forest removal on the regional climate using a detailed three-dimensional energy budget: An application to Africa. *J. Geophys. Res.,* **109,** D21102, doi:10.1029/2003JD004462.

Solomon, S., D. Qin, M. Manning, M. Marquis, K. Averyt, M. M. B. Tignor, H. L. Miller Jr., and Z. Chen, Eds., 2007: *Climate Change 2007: The Physical Sciences Basis*. Cambridge University Press, 996 pp.

Strengers, B. J., and Coauthors, 2010: Assessing 20th century climate–vegetation feedbacks of land-use change and natural vegetation dynamics in a fully coupled vegetation–climate model. *Int. J. Climatol.,* **30,** 2055–2065.

Texier, D., and Coauthors, 1997: Quantifying the role of biosphere-atmosphere feedbacks in climate change: Coupled model simulations for 6000 years BP and comparison with palaeodata for northern Eurasia and northern Africa. *Climate Dyn.,* **13,** 865–881, doi:10.1007/s003820050202.

Thompson, S., B. Govindasamy, A. Mirin, K. Caldeira, C. Delire, J. Milovich, M. Wickett, and D. Erickson, 2004: Quantifying the effects of CO_2-fertilized vegetation on future climate. *Geophys. Res. Lett.,* **31,** L23211, doi:10.1029/2004GL021239.

Thonicke, K., S. Venevsky, S. Sitch, and W. Cramer, 2001: The role of fire disturbance for global vegetation dynamics: Coupling fire into a Dynamic Global Vegetation Model. *Global Ecol. Biogeogr.,* **10,** 661–677.

Tian, Y., R. E. Dickinson, L. Zhou, R. B. Myneni, M. Friedl, C. B. Schaaf, M. Carroll, and F. Gao, 2004: Land boundary conditions from MODIS data and consequences for the albedo of a climate model. *Geophys. Res. Lett.,* **31,** L05504, doi:10.1029/2003GL019104.

Vérant, S., K. Laval, J. Polcher, and M. De Castro, 2004: Sensitivity of the continental hydrologic cycle to the spatial resolution over the Iberian Peninsula. *J. Hydrometeor.,* **5,** 267–285.

Voldoire, A., B. Heickhout, M. Schaeffer, J.-F. Royer, and F. Chauvin, 2007: Climate simulation of the twenty-first century with interactive land-use changes. *Climate Dyn.,* **29,** 177–193.

Wang, G., and E. A. B. Eltahir, 2000a: Biosphere–atmosphere interactions over West Africa. I: Development and validation of a coupled dynamic model. *Quart. J. Roy. Meteor. Soc.,* **126,** 1239–1260.

——, and ——, 2000b: Ecosystem dynamics and the Sahel drought. *Geophys. Res. Lett.,* **27,** 795–798.

——, and ——, 2000c: Role of vegetation dynamics in enhancing the low-frequency variability of the Sahel rainfall. *Water Resour. Res.,* **36,** 1013–1021.

——, ——, J. A. Foley, D. Pollard, and S. Levis, 2004: Decadal variability of rainfall in the Sahel: Results from the coupled GENESIS-IBIS atmosphere–biosphere model. *Climate Dyn.,* **22,** 625–637.

Winter, J. M., J. S. Pal, and E. A. B. Eltahir, 2009: Coupling of Integrated Biosphere Simulator to Regional Climate Model version 3. *J. Climate,* **22,** 2743–2757.

Woodward, F. I., 1987: *Climate and Plant Distribution*. Cambridge Studies in Ecology, Cambridge University Press, 174 pp.

Zeng, N., J. D. Neelin, K. M. Lau, and C. J. Tucker, 1999: Enhancement of interdecadal climate variability in the Sahel by vegetation interaction. *Science,* **286,** 1537–1540.

Zeng, X. B., R. E. Dickinson, A. Walker, M. Shaikh, R. S. DeFries, and J. G. Qi, 2000: Derivation and evaluation of global 1-km fractional vegetation cover data for land modeling. *J. Appl. Meteor.,* **39,** 826–839.